Facile synthesis of stable, water-soluble magnetic CoPt hollow nanostructures assisted by multi-thiol ligands†

Le Trong Lu,[ab] Le Duc Tung,[c] James Long,[d] David Garth Fernig[ef] and Nguyen Thi Kim Thanh*[gh]

Received 6th April 2009, Accepted 26th May 2009
First published as an Advance Article on the web 30th June 2009
DOI: 10.1039/b906839b

We report the synthesis of CoPt hollow nanostructures using a simple reduction method in aqueous solution in the presence of poly(methacrylic acid) pentaerythritol tetrakis (3-mercaptopropionate) (PMAA-PTMP) polymer or a mixture of *O*-[2-(3-mercaptopropionyl-amino)ethyl]-*O′*-methylpolyethylene glycol (PEG-SH) polymer and cysteine-cysteine-alanine-leucine-asparagine-asparagine (CCALNN) peptide ligands. The presence of the multi-thiol functional group of the ligands is essential for the formation of the hollow nanostructures and their perimeter size can be tuned within the range of 7–54 nm by changing peptide concentration or length of polymer. These hollow nanostructures are water-soluble and superparamagnetic at room temperature. They are stable in a wide range of pH from 1 to 10, high electrolyte concentration up to 2 M NaCl, and in cell culture medium which makes them have great potential to be utilised in biomedical applications.

Introduction

Hollow nanostructures have been attracting a great deal of attention because of their high surface area, low density and interesting physical properties,[1] which could be exploited for various applications including catalysis,[2] photothermal treatment,[3] optical imaging,[4] drug delivery[5] and magnetic resonance imaging (MRI).[6]

Recently, much progress has been made on the synthesis of hollow nanostructures with a number of methods developed including those involved hard templates (*e.g.* polymer and silica[7–11]) or soft templates (*e.g.* emulsion droplets,[12–15] surfactants[16] and gas bubbles[17–19]), physical processes based on Kirkendall effect,[20–22] Ostwald ripening,[23–26] self-assembly,[27] oriented attachment,[28] chemically induced self-transformation,[29,30] *etc.* A remaining challenge, however, is how to synthesise the hollow nanostructures suitable for biomedical applications, *i.e.* they have to be soluble and stable in the aqueous solutions and biofunctionalised. In addition, in many cases, the applications also require ultra small hollow nanostructures (*e.g.* with size less than 20 nm) of which it could be very difficult to be realised using conventional synthesis methods in aqueous solution.

Previously, we have successfully fabricated water-soluble magnetic cobalt nanoparticles (NPs). The syntheses were carried out in organic solvent using peptides[31] or thermo-responsive polymers that have switchable solubility between organic and aqueous phases as ligands.[32] More recently, water-soluble Co NPs with controllable size and shape were synthesised directly in aqueous medium[33] and used as MRI contrast enhancers.[34]

In this paper, we report a novel approach for the synthesis of water-soluble magnetic hollow nanostructures exploited the unique properties of polymer, peptide or their mixture as ligands. Here, the ligand itself could act as an in-situ soft template and the hollow nanostructures consist of assemblies of small NPs which are held together by the multi-thiol functional groups of the ligands. The method was primarily applied to the synthesis of CoPt hollow nanostructures, but it could also be extended to the synthesis of hollow nanostructures of FePt and NiPt. The synthesis is one-step and carried out simply in aqueous solution at room temperature.

The perimeter size of the CoPt hollow nanostructures can be tuned between 7 and 54 nm by changing the synthesis conditions such as concentration or length of the ligands. The synthesised CoPt hollow nanostructures are found to be superparamagnetic at room temperature, stable in water with pH in the range from 1 to 10 and NaCl concentration up to 2 M. In addition, the surface of the hollow structures has carboxyl (–COOH), hydroxyl (–OH), or amine ($–NH_2$) groups which would enable conjugation with biological molecules of interest such as proteins, lipids and polysaccharides for biomedical applications.

Experimental

Materials

Cobalt (II) chloride hydrate ($CoCl_2.6H_2O$) 97%, hexachloroplatin(IV) acid hexahydrate ($H_2PtCl_6.6H_2O$), 37% Pt basis

[a]*Department of Chemistry, University of Liverpool, Crown Street, Liverpool, L69 7ZD, UK*
[b]*Institute for Tropical Technology (ITT), Vietnam Academy of Science and Technology (VAST), Vietnam*
[c]*Department of Physics, University of Liverpool, Crown Street, Liverpool, L69 3BX, UK*
[d]*Iota NanoSolutions Ltd, Crown Street, Liverpool, L69 7ZB, UK*
[e]*School of Biological Sciences, University of Liverpool, Crown Street, Liverpool, L69 7ZB, UK*
[f]*Liverpool Institute for Nanoscale Science Engineering and Technology (LINSET), University of Liverpool, Crown Street, Liverpool, L69 7ZB, UK*
[g]*The Davy-Faraday Research Laboratory, The Royal Institution of Great Britain, 21 Albemarle Street, London, W1S 4BS, UK. E-mail: ntk.thanh@ucl.ac.uk*
[h]*Department of Physics & Astronomy, University College London, Crown Street, London, WC1E 6BT, UK*

† Electronic supplementary information (ESI) available: Includes structures of ligands and peptides, TEM images and hysteresis loops. See DOI: 10.1039/b906839b

were purchased from Sigma-Aldrich Ltd, UK. Sodium borohydride ($NaBH_4$) 98% was obtained from VWR Ltd, UK. Peptides including cysteine-cysteine-alanine-leucine-asparagine-asparagine (CCALNN), cysteine-cysteine-valine-valine-valine-threonine (CCVVVT), asparagine-asparagine-leucine-alanine-cysteine-cysteine (NNLACC), cysteine-alanine-leucine-asparagine-asparagine (CALNN) and threonine-leucine-valine-valine-asparagine (TLVVN) were received from Sigma-Genosys Ltd, UK. Methoxypolyethylene glycol acetic acid (PEG-COOH) (molecular weight, M_w = 5,000 g/mol), *O*-[-(3-mercapto-propionylamino)ethyl]-*O′*-methyl-polyethyleneglycol (PEG-SH) (M_w = 5,000 and 20,000 g/mol) were purchased from Fluka Ltd, UK. Water-soluble polymers including poly(methacrylic acid) dodecanethiol (PMAA-DDT) (M_w = 13,500 g/mol), and poly-(methacrylic acid) pentaerythritol tetrakis (3-mercaptopropionate) (PMAA-PTMP) (M_w = 2,000 g/mol) were synthesised at University of Liverpool.[35,36]

Synthesis of the CoPt nanoparticles

CoPt NPs were prepared by reduction of Co^{2+} and Pt^{+4} simultaneously in water in the presence of the ligand(s). In a typical procedure, 0.02 mmol cobalt and 0.04 mmol platinum salts (precursors), and ligand(s) with desired concentration were introduced into a 100 ml two-neck flask sealed with rubber septa, which was then de-gassed by purging with N_2 for 30 min. The flask was then vacuumed for at least 10 min to remove excess N_2, this step is very important to avoid froth forming from the reaction which could hinder the fast injection of $NaBH_4$ and could interfere with the final product. To this flask, degassed and de-ionised water (19 mL) was added and the mixture was sonicated for 10–15 min in a U300 Ultrawave sonic bath (Ultrawave Ltd, UK) to dissolve the stabilising ligand(s) and precursors. $NaBH_4$ solution was freshly prepared by dissolving 0.4 mmol of $NaBH_4$ in degassed water (1 mL). This solution was rapidly injected into the reaction flask under sonication. The final concentrations of $NaBH_4$, $CoCl_2$ and H_2PtCl_6 in the reaction flask were 20, 1 and 2 mM. Sonication was continued for 5 min after the injection. During this time, the solution changed rapidly to a dark near black color with some gas evolution.

Characterisation

The morphology of the NPs was determined using FEI Tecnai G^2 120 kV TEM, operated at 100 kV and visualised using analySIS software. Specimens of CoPt NPs for inspection by TEM were prepared by drop 5 μL of a dilute solution on TEM grid and left to dry under ambient condition. Samples of CoPt NPs were purified by centrifugation at 6,000–12,000 rpm for 10 minutes. Supernatants were discarded, and the sediments were redispersed in water by sonication. The wash was repeated at least two times before preparing for TEM. The diameter (d) of the NPs and their size distribution were taken as the mean of minimum 200 NPs measured from enlarged photographs using Bersoft Image Measurement 1.0 software.

High resolution Transmission Electron Microscopy (HRTEM) was carried out using a JEOL 4000EX II microscope operated at 400 kV with a resolution limit of 0.14 nm. The crystallographic structure of the particles was determined from the Fast Fourier Transform (FFT) image.

The composition of the synthesised sample was analysed using an inductively coupled plasma atomic emission spectroscopy (ICP-AES) (Spectro Ciros^{CCD}).

The hydrodynamic size of the synthesised NPs in different electrolyte and pHs was measured using dynamic light scattering, Zeta-sizer Nano S (Zen 3600), Malvern Instruments Ltd, UK.

Results and discussion

The synthesis was carried out at room temperature upon which a simultaneous reduction of Co^{2+} and Pt^{4+} in water in the presence of ligands produced CoPt NPs. We have used different types of polymers including PMAA-PTMP, PMAA-DDT, PEG-SH and PEG-COOH. The structure of these polymers is shown in Fig. S1, ESI.† The hollow nanostructures were formed in the presence of the PMAA-PTMP polymer containing multi-thiol group (Fig. 1a).

For the synthesis in the presence of PMAA-DDT (mono-thiolether), PEG-COOH (no-thiol) or PEG-SH (mono-thiol), solid NPs or nanochains were obtained (Fig. S3, ESI†).

In order to confirm that the presence of the multi-thiol functional group plays an important role in the formation of the hollow nanostructures, we have extended our investigation further by using peptides as ligands. We have used CCALNN, CCVVVT and NNLACC peptides which have di-thiol functional groups and compared them with CALNN, which has a single thiol and TLVVN that lacks a thiol (see peptide structures, Fig. S2, ESI†). In the presence of these peptides, only aggregated NPs were produced, which then precipitated in the aqueous solution. These peptides are short in length, and as a result, when coating the NPs, may not give enough steric repulsion to stabilise NPs. Moreover, the other functional groups of the peptides (*i.e.* amine, amide and caboxyl) may have bridged NPs and caused them to aggregate.

In order to overcome this problem, a mixture of peptide and polymer (*e.g.* PEG-SH, M_w = 5,000 g/mol) was investigated. When di-thiol peptide CCALNN, CCVVVT or NNLACC was used in conjunction with the polymer, CoPt hollow nanostructures were obtained. Fig. 1b shows an example of hollow nanostructures obtained when using CCALNN. On the other hand, solid NPs and nanochains were obtained in the presence of mono-thiol CALNN and non-thiol TLVVN, respectively

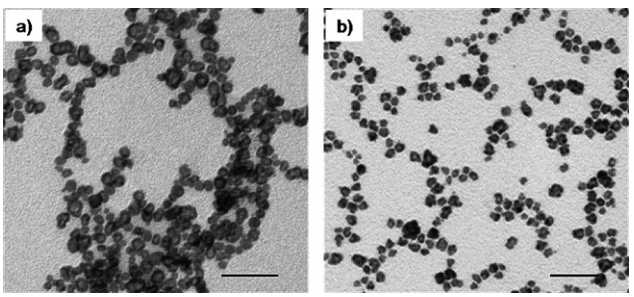

Fig. 1 TEM images of the CoPt hollow nanostructures synthesised in the presence of different ligands: a) 0.24 mM PMAA-PTMP; b) 0.12 mM PEG-SH and 0.12 mM CCALNN. Scale bar: 50 nm.

(Fig. S4, ESI†). Thus, the presence of the multi-thiol functional group in the peptides is very important for the formation of the CoPt hollow nanostructures, whereas the mono-thiol PEG-SH is critical in this instance for ensuring colloidal stability.

The perimeter size of the hollow nanostructures can be controlled by changing concentration and the molecular weight, M_w, (or length) of the ligands. The studies were carried out for the mixture of di-thiol peptide CCALNN and the polymer PEG-SH. The CCALNN concentration was varied from 0.06 to 0.96 mM. On the other hand, for PEG-SH polymer, its concentration is fixed at 0.24 mM but the molecular weight can be chosen between 5,000 and 20,000 g/mol. It was observed that hollow nanostructures were formed rather homogenously when CCALNN concentration is from 0.12 to 0.24 mM. At 0.12 mM, the average perimeter size of the hollow nanostructures was 9.8 ± 1.3 (Fig. 2a) and 14.6 ± 1.9 nm (Fig. 2b) for PEG-SH with M_w = 5,000 and 20,000 g/mol, respectively. At 0.24 mM, these values increased correspondingly to 14.9 ± 3 and 18.8 ± 3.4 nm (Fig. S5b and S5e, ESI†). Thus, it appears that the perimeter size of the CoPt hollow nanostructures increases with either the increasing of peptide CCALNN concentration or the molecular weight (or length) of the polymer PEG-SH.

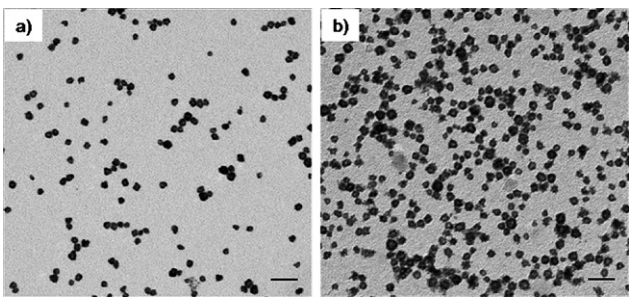

Fig. 2 TEM images of the CoPt hollow nanostructures synthesised in the presence of 0.12 mM CCALNN and 0.24 mM PEG-SH with molecular weight (M_w) of: a) 5,000 and b) 20,000 g/mol; Scale bar: 50 nm.

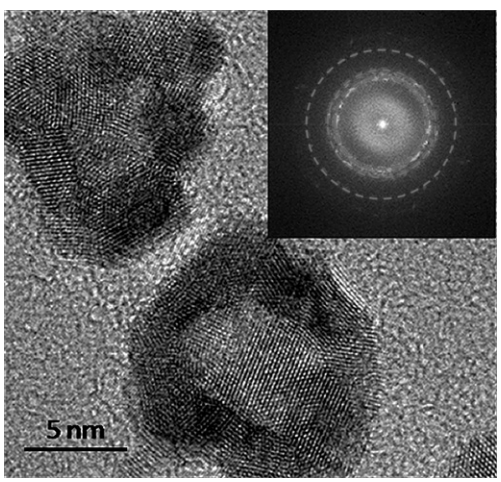

Fig. 3 HRTEM image of the CoPt hollow nanostructures synthesised in the presence of 0.12 mM CCALNN and 0.24 mM PEG-SH (Mw = 5,000 g/mol). The inset shows the corresponding Fast Fourier Transform (FFT) image which shows 3 strongest rings with d-spacings of 2.213, 1.954 and 1.362 Å.

To study in more detail, HRTEM was performed on the hollow nanostructures synthesised in the presence of 0.12 mM CCALNN and 0.24 mM PEG-SH (M_w = 5,000 g/mol) and the result was shown in Fig. 3. It can be seen that the hollow nanostructures consist of crystallised small NPs with a size of about 3 nm. At the edge of the hollow nanostructures, the mass contrast is darker than inside, which suggests the presence of small NPs around the outer ring. From the FFT image, one can observe 3 rings with d-spacings of 2.213, 1.954 and 1.362 Å which are closely matched with the d spacings of the corresponding (100), (200) and (220) planes of the fcc $CoPt_3$ phase (No 29–0499).

When the CCALNN concentration is outside the 0.12–0.24 mM range, other than the hollow nanostructures, different morphologies of the as-synthesised NPs were obtained. For PEG-SH with molecular weight M_w = 5,000 g/mol, we found that its mixture with 0.06 mM of CCALNN resulted in an inhomogeneous sample containing hollow nanostructures with average perimeter size of 7.3 ± 1.5 nm and other discrete small NPs (Fig. S5a, ESI†). In this case, the number of di-thiols is presumably too low and, as a result, only part of the population of small NPs in the solution can be bridged to form hollow nanostructures. At CCALNN concentrations of 0.6 and 0.96 mM, hollow porous-like nanostructures with corresponding average perimeter size of 30.5 ± 8.5 nm and 40 ± 7.9 nm were obtained (Fig. S5c and S5d, ESI†). When the PEG-SH with molecular weight M_w = 20,000 g/mol were used with 0.96 mM of CCALNN, the average perimeter size of the hollow nanostructures increases to 54 ± 8.6 nm (Fig. S5f, ESI†).

We have also investigated the effect of the ratio of metal salt precursors. Here, we have used the mixture of CCALNN (0.12 mM) and PEG-SH (0.24 mM, M_w = 5,000 g/mol). It was found that the hollow nanostructures were formed rather homogenously when the ratio of Co/Pt salts was 1:2 (Fig. 2a) and 3:1 (Fig. S6a, ESI†). At higher ratios (9:1) there are no hollow nanostructures and the sample contained only small NPs (Fig. S6b, ESI†). When only Pt salt was used, a large network of small NP aggregates was formed (Fig. S6c, ESI†). Thus, it is also clear that the hollow nanostructures are formed only in the presence of both Co and Pt salts and in a certain range of their concentrations.

The composition of the as-synthesised CoPt NPs can be tuned by changing the concentration of starting materials and the data is listed in table 1. It is interesting to see that the composition of the hollow nanostructures is closely followed with the starting Co:Pt salt ratio when it is 1:2, 1:1 and 3:1. In an isostructural FePt system synthesised using the thermodecomposition of $Fe(CO)_5$ and reduction of Pt (II) acetylacetonate ($Pt(acac)_2$), it was found that the composition is dependent on the size of the synthesised NPs.[37]

The magnetic properties of the CoPt hollow nanostructures were investigated by measuring the zero-field-cooled (ZFC) and field-cooled (FC) magnetisation. The investigation was carried out for the samples synthesised under the same 1:2 ratio of precursors Co and Pt salts in the presence of PEG-SH (0.24 mM) and different concentrations of CCALNN from 0.06 to 0.96 mM. It can be seen from Fig. 4 that all samples show a maximum in the ZFC curve, which is due to the transition of the NPs from the superparamagnetic to ferromagnetic blocked state with

Table 1 The dependence of composition and morphology of CoPt NPs on precursor ratio

Sample	Co salt concentration (mM)	Pt salt Concentration (mM)	Starting Co:Pt ratio	Composition of synthesised NPs[a]	Morphology
1	0	3	0:3	Pt	small NPs, large network
2	1	2	1:2	$CoPt_{1.74}$	hollow structures
3	1.5	1.5	1:1	$Co_{1.2}Pt$	hollow structures
4	2.25	0.75	3:1	$Co_{3.5}Pt$	hollow structures
5	2.7	0.3	9:1	$Co_{20.7}Pt$	small NPs

[a] The composition was obtained by ICP-AES.

decreasing temperature. The blocking temperature, T_B, increases from 14 K to 175 K as the perimeter size of the nanostructure increases from 7.3 to 40 nm.

In contrast to the ZFC curves shown in Figs. 4b,c,d,e, Fig. 4a shows a maximum at about 14 K followed by a small shoulder at around 50 K. This feature is consistent with the inhomogeneity of the sample as seen from the TEM image (Fig. S5a, ESI†). Here, the maximum at 14 K may be attributed to the presence of small NPs of around 3 nm in the sample and the shoulder at 50 K by hollow nanostructures with larger perimeter size of 7.3 ± 1.5 nm.

For two samples with CCALNN concentrations of 0.12 mM (Fig. 4b) and 0.24 mM (Fig. 4c), the splitting between the ZFC and FC curves occurs at temperatures quite close to T_B, suggesting that the hollow nanostructures are of good homogeneity and monodispersity to be consistent with those seen in the TEM images (Fig. 2a and Fig. S5b, ESI†).

The hysteresis loops of the samples measured at 5 K were presented in Fig. S7, ESI.† The coercivity obtained are 550, 800, 470, 1020 and 890 Oe, for samples with the average size of 7.3, 9.8, 14.9, 30.5, and 40 nm.

To assess the usefulness of the hollow NPs for biomedical applications, the examination of stability was carried out. The hollow NPs were seen to be colloidally stable in aqueous solution for at least five months after the synthesis. Even after removal of access free ligands by three centrifugations (12,000 rpm, 10 min), the CoPt hollow nanostructures were still very well dispersed and stable in solution, whereas with Co NPs synthesised in water, this step would cause them to aggregate.[33]

At different electrolyte (NaCl) concentrations and pH values, the hydrodynamic size of the hollow nanostructures, *i.e.* the core plus the polymer coating, can be measured using dynamic light scattering technique and the results are presented in Fig. 5 for the synthesis under a mixture of PEG-SH (0.24 mM) and CCALNN (0.12 mM). As for NaCl concentrations up to 2 M, the hydrodynamic size keeps almost unchanged at 20 nm indicating that the hollow nanostructures are not aggregate but remain well dispersed and stable in the solution. Similarly, when the pH

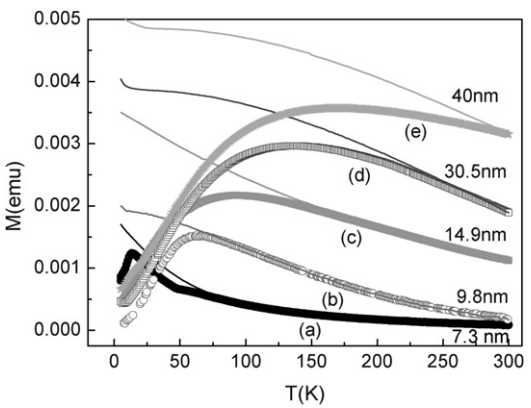

Fig. 4 ZFC (symbols) and FC (lines) curves of CoPt hollow nanostructures synthesised in the presence of mixture of 0.24 mM PEG-SH (5000 g/mol) and different CCALNN concentration: a) 0.06 mM, b) 0.12 mM, c) 0.24 mM, d) 0.60 mM and e) 0.96 mM.

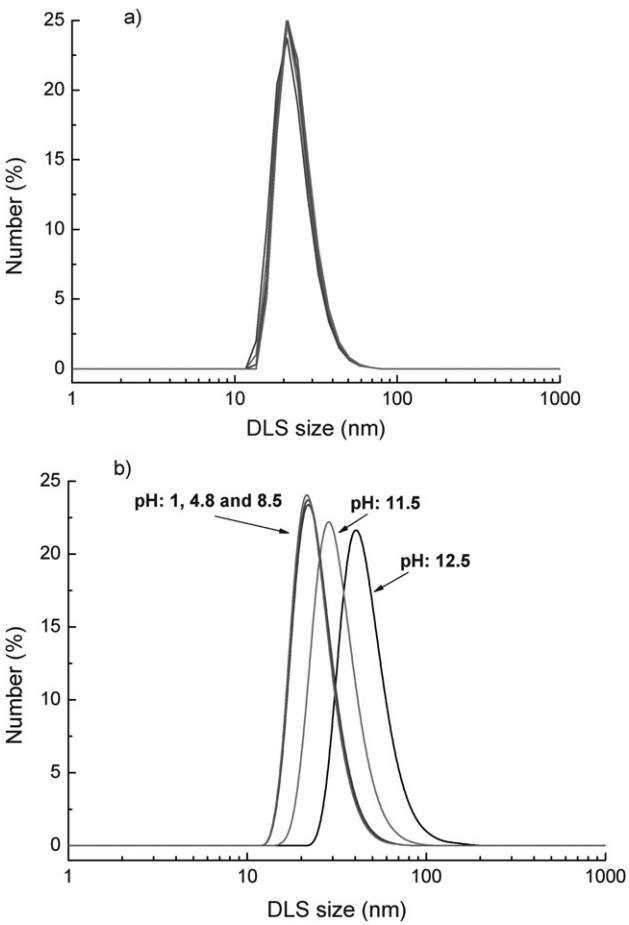

Fig. 5 Hydrodynamic size distribution of CoPt hollow nanostructures at a) different NaCl concentrations of 0, 200, 300, 0.8, 1.6 and 2 M and b) different pHs of 1, 4.8, 8.5, 11.5 and 12.5.

increases from 1 to 8.5, the hydrodynamic size also remained constant at 20 nm, but then it increased to 25 nm at pH 11.5 and 38 nm at pH 12.5. At pH > 11.5, all carboxylic groups at the terminals of the peptides have negative charge, which would cause repulsion of neighbouring peptide molecules. This would destabilise the highly compacted self assembled monolayer of ligands which is required for stabilisation of NPs.[38] Since no precipitation was observed in the solution the large increases in the hydrodynamic size may also be that the PEG ligand shell extended in straight conformation rather curling up in a shorter form.

The stability of the sample in cell culture medium, Dulbecco's Modified Eagles Medium (DMEM), was also studied. DLS measurements were carried out, but cell culture medium has very complex composition that obscures the nanoparticle peaks. However, no precipitation or aggregate of the NPs was visually observed which may suggest that the hollow nanostructures remained stable and soluble in the medium.

The versatility of the synthesis method for hollow structures using multi-thiol funtional ligand was preliminarily studied also for isostructural FePt and NiPt systems. With a mixture of CCALNN (0.12 mM) and PEG-SH (0.24 mM, M_w = 5,000), hollow nanostructures were also formed in both FePt and NiPt systems (Fig. S8, ESI†), although they are not so monodispersed and there are also small NPs present in the samples. Nevertheless, the results would indicate that our simple approach may be made more general to other systems as well.

Given the fact that the hollow structures were formed only with polymer PMAA-PTMP or peptides containing multi-thiol and not with single or non-thiolated ligands, it is clear that the multi-thiol functional group present in these ligands play a very important role. The thiol functional group is well known to bind strongly with noble metals like Au or Pt.[39,40] In our synthesis, it was found that the hollow nanostructures consist of small NPs. Since each small particle was coated by the ligand, the multi-thiol functional group itself could act as a "glue" in the process of forming the hollow structures. The long ligand (*e.g.* PMAA or PEG), on the other hand, has two different roles. Firstly, it can act as a soft template to assist the formation of the hollow nanostructure; secondly, by virtue of its size, it will provide steric and/or electrostatic repulsion strong enough to protect the hollow nanostructures from aggregating. The proposed mechanism involving the multi-thiol functional group in the formation of the hollow nanostructures is presented in Scheme 1. Accordingly, to realise the formation of the hollow nanostructures, there should be sufficient content of Pt in respect to that of Co.

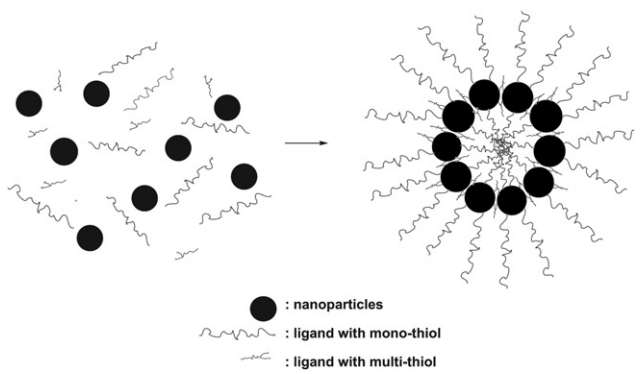

Scheme 1 Proposed mechanism of hollow formation of CoPt NPs.

When the Pt content was too low (*e.g.*, 10% in molarity), the number of thiols bound on each individual particle is also low and that makes it difficult for the small solid NPs to be held together and as a result only small NPs were formed (Fig. 6Sb, ESI†). On the other hand, when Pt content was high (*e.g.*, 100%), too much thiol was present on the surface of small NPs which resulted in the formation of aggregated solid NPs (Supplementary Fig. 6Sc, ESI†).

Conclusions

In summary, a facile synthesis in water and at room temperature has been developed for CoPt hollow nanostructures. The formation of the hollow structures was assisted by the presence of multi-thiol functional group of the ligand. The perimeter size of the CoPt hollow nanostructures can be tuned and they are stable under high electrolyte concentration and a wide range of pH values that could make them usable for biomedical applications, water purification for environmental cleaning.

Acknowledgements

Nguyen T.K. Thanh thanks the Royal Society for her University Research Fellowship. Le T. Lu thanks Vietnamese Government for his PhD studentship (322 project). David G. Fernig is funded by the North West Cancer Research Fund and the Cancer and Polio Research Fund. The authors thank Andrew Ian Cooper and Bien Tan for supplying PMAA-PTMP and PMAA-DDT polymers and Ian Prior, for provision of the TEM facilities.

References

1 S. E. Skrabalak, L. Au, X. D. Li and Y. Xia, *Nat. Protocol.*, 2007, **2**, 2182–2190.
2 S. W. Kim, M. Kim, W. Y. Lee and T. Hyeon, *J. Am. Chem. Soc.*, 2002, **124**, 7642–7643.
3 J. Y. Chen, D. L. Wang, J. F. Xi, L. Au, A. Siekkinen, A. Warsen, Z. Y. Li, H. Zhang, Y. N. Xia and X. D. Li, *Nano Lett.*, 2007, **7**, 1318–1322.
4 J. Chen, F. Saeki, B. J. Wiley, H. Cang, M. J. Cobb, Z. Y. Li, L. Au, H. Zhang, M. B. Kimmey, X. D. Li and Y. Xia, *Nano Lett.*, 2005, **5**, 473–477.
5 D. E. Bergbreiter, *Angew. Chem., Int. Ed.*, 1999, **38**, 2870–2872.
6 J. H. Gao, G. L. Liang, J. S. Cheung, Y. Pan, Y. Kuang, F. Zhao, B. Zhang, X. X. Zhang, E. X. Wu and B. Xu, *J. Am. Chem. Soc.*, 2008, **130**, 11828–11833.
7 H. Zhou, T. X. Fan and D. Zhang, *Microporous Mesoporous Mater.*, 2007, **100**, 322–327.
8 J. Wang, K. P. Loh, Y. L. Zhong, M. Lin, J. Ding and Y. L. Foo, *Chem. Mater.*, 2007, **19**, 2566–2572.
9 N. Du, H. Zhang, J. Chen, J. Y. Sun, B. D. Chen and D. R. Yang, *J. Phys. Chem. B*, 2008, **112**, 14836–14842.
10 Y. P. Zhang, Y. Chu and L. H. Dong, *Nanotechnology*, 2007, **18**, 435608–435612.
11 M. Ohnishi, Y. Kozuka, Q. L. Ye, H. Yoshikawa, K. Awaga, R. Matsuno, M. Kobayashi, A. Takahara, T. Yokoyama, S. Bandow and S. Iijima, *J. Mater. Chem.*, 2006, **16**, 3215–3220.
12 Z. X. Wang, M. Chen and L. M. Wu, *Chem. Mater.*, 2008, **20**, 3251–3253.
13 Q. Liu, H. J. Liu, M. Han, J. M. Zhu, Y. Y. Liang, Z. Xu and Y. Song, *Adv. Mater.*, 2005, **17**, 1995–1999.

14 Z. Y. Jiang, Z. X. Xie, X. H. Zhang, S. C. Lin, T. Xu, S. Y. Xie, R. B. Huang and L. S. Zheng, *Adv. Mater.*, 2004, **16**, 904–907.
15 X. J. Zhang and D. Li, *Angew. Chem., Int. Ed.*, 2006, **45**, 5971–5974.
16 D. B. Zhang, L. M. Qi, J. M. Ma and H. M. Cheng, *Adv. Mater.*, 2002, **14**, 1499–1502.
17 L. Guo, F. Liang, X. G. Wen, S. H. Yang, L. He, W. Z. Zheng, C. P. Chen and Q. P. Zhong, *Adv. Funct. Mater.*, 2007, **17**, 425–430.
18 H. W. Hou, Q. Peng, S. Y. Zhang, Q. X. Guo and Y. Xie, *Eur. J. Inorg. Chem.*, 2005, 2625–2630.
19 Q. Peng, Y. J. Dong and Y. D. Li, *Angew. Chem., Int. Ed.*, 2003, **42**, 3027–3030.
20 Y. D. Yin, R. M. Rioux, C. K. Erdonmez, S. Hughes, G. A. Somorjai and A. P. Alivisatos, *Science*, 2004, **304**, 711–714.
21 S. Peng and S. H. Sun, *Angew. Chem., Int. Ed.*, 2007, **46**, 4155–4158.
22 A. Cabot, V. F. Puntes, E. Shevchenko, Y. Yin, L. Balcells, M. A. Marcus, S. M. Hughes and A. P. Alivisatos, *J. Am. Chem. Soc.*, 2007, **129**, 10358–10360.
23 H. G. Yang and H. C. Zeng, *J. Phys. Chem.*, 2004, **108**, 3492–3495.
24 W. S. Wang, L. Zhen, C. Y. Xu, B. Y. Zhang and W. Z. Shao, *J. Phys. Chem. B*, 2006, **110**, 23154–23158.
25 X. Wang, F. L. Yuan, P. Hu, L. J. Yu and L. Y. Bai, *J. Phys. Chem. C*, 2008, **112**, 8773–8778.
26 B. Liu and H. C. Zeng, *Small*, 2005, **1**, 566–571.
27 A. M. Cao, J. S. Hu, H. P. Liang and L. J. Wan, *Angew. Chem., Int. Ed.*, 2005, **44**, 4391–4395.
28 T. He, D. R. Chen, X. L. Jiao, Y. Y. Xu and Y. X. Gu, *Langmuir*, 2004, **20**, 8404–8408.
29 H. P. Liang, H. M. Zhang, J. S. Hu, Y. G. Guo, L. J. Wan and C. L. Bai, *Angew. Chem., Int. Ed.*, 2004, **43**, 1540–1543.
30 Y. Vasquez, A. K. Sra and R. E. Schaak, *J. Am. Chem. Soc.*, 2005, **127**, 12504–12505.
31 N. T. K. Thanh, V. F. Puntes, L. D. Tung and D. G. Fernig, *J Phys.: Conf. Ser.*, 2005, **17**, 70–76.
32 I. Robinson, C. Alexander, L. T. Lu, L. D. Tung, D. G. Fernig and N. T. K. Thanh, *Chem. Commun.*, 2007, 4602–4604.
33 L. T. Lu, L. D. Tung, I. Robinson, D. Ung, B. Tan, J. Long, A. I. Cooper, D. G. Fernig and N. T. K. Thanh, *J. Mater. Chem.*, 2008, **18**, 2453–2458.
34 L. M. Parkes, R. Hodgson, L. T. Lu, L. D. Tung, I. Robinson, D. G. Fernig and N. T. K. Thanh, *Contrast Media & Molecular Imaging*, 2008, **3**, 150–156.
35 I. Hussain, S. Graham, Z. X. Wang, B. Tan, D. C. Sherrington, S. P. Rannard, A. I. Cooper and M. Brust, *J. Am. Chem. Soc.*, 2005, **127**, 16398–16399.
36 Z. X. Wang, B. E. Tan, I. Hussain, N. Schaeffer, M. F. Wyatt, M. Brust and A. I. Cooper, *Langmuir*, 2007, **23**, 885–895.
37 D. Ung, L. D. Tung, G. Caruntu, D. Delaportas, I. Alexandrou, I. A. Prior and N. T. K. Thanh, *CrystEngComm*, 2009, DOI: 10.1039/b823290n.
38 L. Duchesne, D. Gentili, M. Comes-Franchini and D. G. Fernig, *Langmuir*, 2008, **24**, 13572–13580.
39 M. Brust, M. Walker, D. Bethell, D. J. Schiffrin and R. Whyman, *J. Chem.Soc. Chem. Commun.*, 1994, 801–802.
40 X. Y. Fu, Y. Wang, N. Z. Wu, L. L. Gui and Y. Q. Tang, *J. Colloid Interf. Sci.*, 2001, **243**, 326–330.

